Carrier Wave Shocking of Femtosecond Optical Pulses

R. G. Flesch, A Pushkarev and J. V. Moloney
Arizona Center for Mathematical Sciences
Department of Mathematics
University of Arizona
(Dated: October 5, 2003)

Numerical integration of Maxwell's equations for propagation of a femtosecond pulse in a medium with linear Lorentz response and a Kerr nonlinearity shows shock formation on the underlying carrier wave prior to the envelope shock. The carrier shock is characterized by the appearance of a strong third harmonic pulse whereas the envelope shock appears later as spectral broadening and modulation of the fundamental and higher harmonic spectral features.

Advances in laser technology in the past decade have made possible the production of pulses which contain a few optical cycles [1]. Although such ultrashort pulses contain small amounts of optical energy, enormous intensities exceeding one terawatt/cm^2 can arise and the accompanying intensity-dependent corrections to the index of refraction are such that one can expect novel nonlinear phenomena such as shock formation over very short propagation lengths. Evidence for shock formation on the pulse envelope has already been seen experimentally [2] and can be quantitatively understood using standard envelope approximations [3] to Maxwell's equations. Laser-induced breakdown (LIB) cannot be ruled out at such very high peak intensities but there is evidence to show that for such short and hence low energy pulses, the cascade-avalanche path to breakdown is unlikely and multi-photon processes are more likely to lead to breakdown [4]. Moreover breakdown becomes a sensitive function of optical wavelength. Shock formation on the carrier wave is likely to compete with other physics during the critical collapse of femtosecond duration optical pulses in optically transparent media where the local intensity at the critical collapse distance can become very large.

In this letter we confine our attention to plane wave propagation for simplicity and show that an optical carrier shock can arise in a medium with an instantaneous Kerr nonlinearity. Dispersion plays an important role in shock regularization (smoothing) and influences the signature of the carrier shock. As dispersion is typically strong for such short optical pulses (the dispersion length scales as $\frac{k''}{\tau_p^2}$, where k'' is the leading order contribution to the group velocity dispersion (GVD) and τ_p is the characteristic pulse length), phase matching can easily be achieved for third harmonic and higher harmonic generation leading to the separation in time of a strong third harmonic optical pulse moving with a different group velocity from the fundamental. For very weak dispersion, a component of the third harmonic pulse moves with the fundamental and in the dispersionless case, all higher harmonics of the fundamental are phase-matched and see explosive growth. As the phenomena we are concerned with occurs on the scale of the carrier wavelength, no envelope approximations are valid and one must resort to a numerical integration of Maxwell's equations. Numerical schemes for the integration of Maxwell's equations have been refined in the past few years [5] – [8] to allow for an efficient integration of media with both memory in the linear and nonlinear polarizations.

We restrict our attention to nonmagnetic dielectric media with no free charges in which case we have for Maxwell's equations

$$\frac{\partial B_y}{\partial t} = \frac{\partial E_x}{\partial z} \quad , \quad \frac{\partial D_x}{\partial t} = \frac{1}{\mu_0}\frac{\partial B_y}{\partial z} \ , \tag{1}$$

where all quantities above and in the following are in MKS units. The medium is modeled by a single Lorentz oscillator plus an instantaneous Kerr nonlinearity

$$D_x(z,t) = \epsilon_0 \Bigg\{ \varepsilon_\infty E_x(z,t) \ + \ \int_{-\infty}^{t} dt' \chi(t-t') E_x(z,t') + \ \chi^{(3)} E_x^3(z,t) \Bigg\} \ , \tag{2}$$

with the linear susceptibility given by

$$\begin{aligned} \chi(t) \ &= \ \frac{\omega_p^2}{\sqrt{\omega_0^2 - \delta^2/4}} e^{-\delta t/2} \sin(\sqrt{\omega_0^2 - \delta^2/4}\, t) \\ \hat{\chi}(\omega) \ &= \ \frac{\omega_p^2}{\omega_0^2 - i\delta\omega - \omega^2} \ , \end{aligned} \tag{3}$$

and $\omega_p^2 = (\varepsilon_s - \varepsilon_\infty)\omega_0^2$, ε_s and ε_∞ the static and infinite relative permittivities respectively and ω_0 the resonance frequency of the Lorentz oscillators. Maxwell's equations are solved by either a second-order in time, second order in space [(2,2)] FD-TD method [9] or a second-order in time, fourth order in space [(2,4)] scheme [10] The numerical dispersion inherent in these methods has recently received a good deal of attention [11, 12] and we have chosen our spatial discretizations accordingly. Controlling the numerical dispersion is of particular importance when no physical dispersion is present and when high frequencies are present due to shock formation. We have made use of both differencing techniques and successive refinements of our spatial grid to confirm our results.

The convolution integral $P_L = \epsilon_0 \int dt' \ \chi(t-t') \ E_x(t')$ in Eq. 2 is solved by a method first suggested by Jackson [13] and more recently put into practice for Lorentz

models in references [5]– [8]. Due to the simple form chosen for the linear susceptibility one can easily derive the following second order ordinary differential equation,

$$\frac{1}{\omega_0^2}\frac{d^2P_L}{dt^2} + \frac{\delta}{\omega_0^2}\frac{dP_L}{dt} + P_L = \frac{\omega_p^2}{\omega_0^2}\epsilon_0 E_x \ . \tag{4}$$

which is solved by second-order central differencing.

Ignoring dispersion initially we obtain a prediction for the carrier shock formation time. For this case and for later analysis it is useful to recast the coupled equations as a second-order integro-differential equation

$$\frac{\partial^2 E_x}{\partial t^2} - \varepsilon_\infty c^2 \frac{\partial^2 E_x}{\partial z^2} - \chi^{(3)}\frac{\partial^2 E_x^3}{\partial t^2} - \frac{\partial^2 P_L}{\partial t^2} = 0 \ , \tag{5}$$

where c is the speed of light in vacuum. Closely connected with Eq. 5 in the case of zero dispersion ($P_L = 0, \varepsilon_\infty = 1$) is the following transport equation

$$\frac{\partial E_x}{\partial t} - C(E_x)\frac{\partial E_x}{\partial z} = 0 \ , \tag{6}$$

with the amplitude-dependent velocity $C(E_x)$ given by

$$C(E_x) = \frac{c}{\sqrt{1+3\chi^{(3)}E_x^2}} \ . \tag{7}$$

Using Eq. 7 and its first time derivative to eliminate all time derivatives in Eq. 5 (with $P_L = 0$) one can show that any solution of Eq. 6 is a solution of the Maxwell Eq. 5. Since Eq. 6 is known to have shock solutions [14] one might expect the same to be true of the corresponding Maxwell's equation. Given an initial condition $E_x(z,0)$ for Eq. 6, one can show [14] that the time for the wave to break is given by

$$t_B = -\left(\frac{d}{d\xi}F(\xi)\bigg|_{\xi=\xi_B}\right)^{-1} \ , \tag{8}$$

where $F(\xi) \equiv C[E_x(\xi,0)]$ and ξ_B denotes the value of ξ for which $F'(\xi) < 0$ and $|F'(\xi)|$ is a maximum.

We now show that in the absence of dispersion, integration of the system Eqs. 1 , 4 leads to carrier shock formation and that the numerically-determined breaking times are in good agreement with Eq. 8. As an initial condition we choose a 30 fs Gaussian pulse (FWHM) of amplitude E_0 and carrier frequency $\omega_c = 4.0 \times 10^{14} (T_{opt} = 15.7\text{fs})$. The Kerr medium used has a dimensionless strength $\chi^{(3)}E_0^2 = 0.02214$. In Fig. 1 we show the pulse profile shortly after having entered the Kerr medium and a second profile (solid) after the pulse has propagated 20 microns. Carrier shock formation is clearly evident, the strongest shock occurring where the pulse has maximum amplitude. The spatial Fourier transform shows the presence of multiple harmonics due to exact phase matching for this dispersionless medium. We emphasize that the initial condition *was not chosen* to satisfy Eq. 6 and hence formation of a shock is not a trivial consequence of the correspondence between Eq. 6 and Eq. 5.

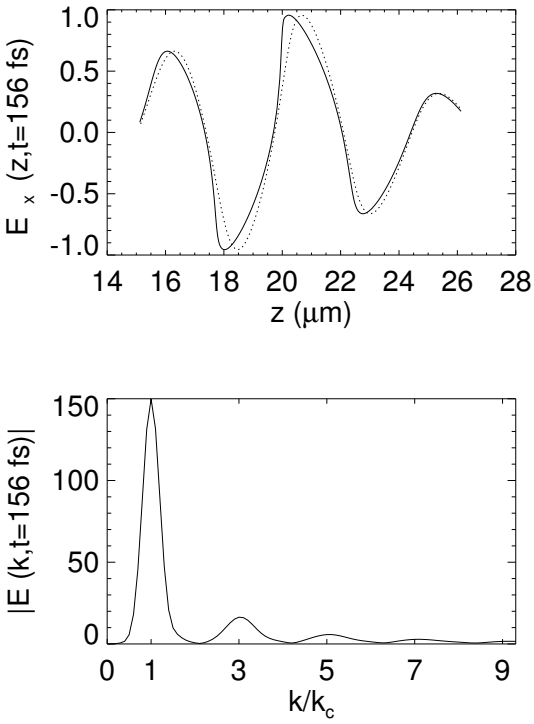

FIG. 1: A 30 fs pulse after propagating 6.8 (dotted) and 20.2 (solid) microns in a dispersionless medium with Kerr nonlinearity 0.022. The dotted curve has been translated so as to coincide with the breaking waveform.

By examining a movie of closely spaced snapshots like those presented in Fig. 1, one can estimate the time for wave breaking. In Fig. 2 we present many such numerically-determined breaking times for different values of the dimensionless Kerr strength $\chi^{(3)}E_0^2$. The pulse initial conditions were the same as above. The solid line is the curve determined by inserting our initial condition into Eq. 8 which yields

$$\begin{aligned} T_B^c &= \frac{1}{3\pi}\frac{T_{opt}}{\chi^{(3)}E_0^2}\frac{(1+4.5\chi^{(3)}E_0^2)^{3/2}}{\sqrt{(1+3\chi^{(3)}E_0^2)(1+6\chi^{(3)}E_0^2)}} \\ &\xrightarrow[\chi^{(3)}E_0^2\to 0]{} \frac{1}{3\pi}\frac{T_{opt}}{\chi^{(3)}E_0^2} \ . \end{aligned} \tag{9}$$

In arriving at Eq. 9 we have assumed that the pulse width T_{FWHM} is longer than the optical period T_{opt}. The agreement between the numerical values and Eq. 9 is quite good for the all but the largest values of $\chi^{(3)}E_0^2$. The deviation for larger values can in part be attributed to the fact that the predicted values assume that the pulse is always in the Kerr medium whereas in the numerical simulations the pulse enters from vacuum. For larger Kerr strengths the breaking occurs so rapidly that this difference is important.

Great care was taken to insure that the breaking times are not an artifact of the numerical dispersion. To this

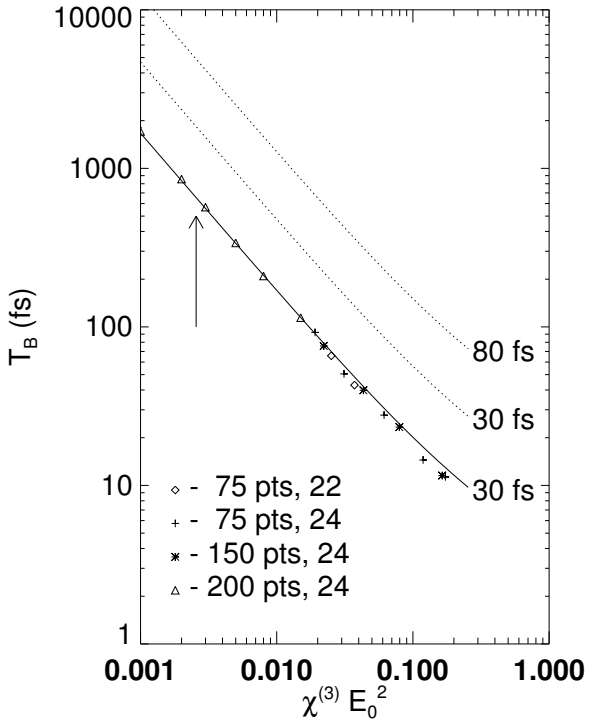

FIG. 2: Numerically determined breaking times as a function of the nonlinearity. Different symbols denote different spatial resolutions and use of either the (2,2) or (2,4) numerical scheme. The formulae in Eqs. 9 and 11 are represented by the solid and dotted lines respectively for the pulse widths indicated.

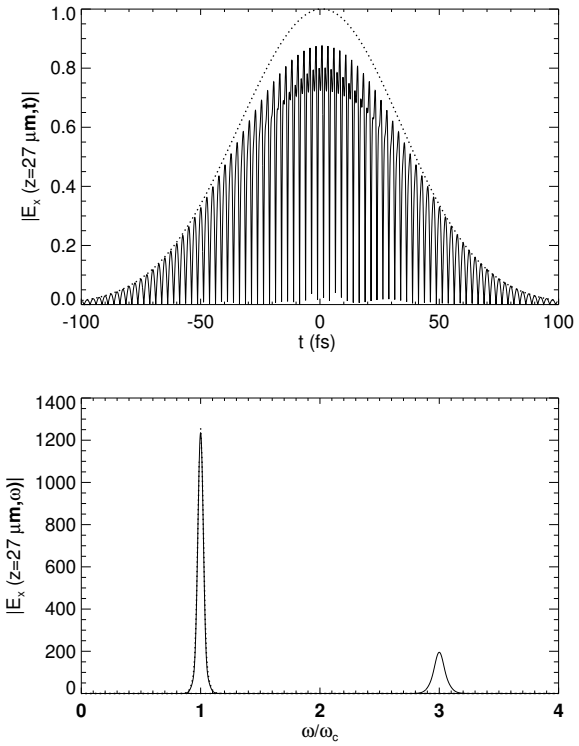

FIG. 3: Comparison of the envelope approximation with the 1D Maxwell's equation after propagating 27 microns. The appearance of the strong third harmonic in the Maxwell spectrum indicates the presence of a carrier shock. Note that the Fourier transform for the envelope has been shifted by ω_c to facilitate comparison.

end a relatively large number of points per wavelength were used. In addition, both the (2,2) and (2,4) numerical schemes were used and as one can see in the Fig. 2 the results do not depend on scheme or discretization.

To contrast carrier shock formation with the more well known envelope shock formation [1, 3], we outline the derivation of the envelope breaking time in terms of our variables. Inserting the standard envelope approximation $E_x(z,t) = E_0(Ae^{i(k_c z-\omega_c t)} + c.c)$ into Eq. 5 one obtains

$$\begin{aligned}\frac{\partial A}{\partial z} &= -k_c'\frac{\partial A}{\partial t} - \frac{ik_c''}{2}\frac{\partial^2 A}{\partial t^2} + \frac{k_c'''}{6}\frac{\partial^3 A}{\partial t^3} + \chi^{(3)}E_0^2\frac{3i\omega_c^2}{2k_c c^2}|A|^2 A \\ &- \chi^{(3)}E_0^2\frac{\omega_c}{2k_c c^2}\left(2-\omega_0\frac{k_c'}{k_c}\right)\frac{\partial |A|^2 A}{\partial t}\ , \end{aligned} \tag{10}$$

where $k_c^2c^2 = \omega_c^2 n(\omega_c) = \omega_c^2[1+\hat{\chi}(\omega_c)]$ and primes denote derivatives with respect to ω. The last term in Eq. 10 gives rise to the envelope shock. One can explicitly derive an envelope breaking time if the GVD term (k_c'') is small relative to the shock term. If one completely neglects the GVD term, transforms into a frame moving with the group velocity and separates real and imaginary parts with $A = \sqrt{I}\exp(i\phi)$, one arrives at a nonlinear wave equation for the dimensionless intensity I similar to Eq. 6 which describes the breaking of the envelope. Using the same analysis which leads to Eq. 9 we obtain

$$T_B^e = \frac{0.156}{\chi^{(3)}E_0^2}\frac{c}{v_p}\frac{1}{2-v_p/v_g}T_{FWHM}\ , \tag{11}$$

where v_p and v_g are the phase and group velocities at the carrier frequency. In physically relevant situations $\chi^{(3)}E_0^2 \ll 0.1$ and hence we may use the approximation on the right-hand side of Eq. 9 to obtain the following simple ratio for the carrier and envelope breaking times

$$\frac{T_B^e}{T_B^c} \approx 1.467\frac{T_{FWHM}}{T_{opt}} \tag{12}$$

where we have taken $v_p = v_g = c$ due to the small dispersion. Since the envelope approximation is only valid when the pulse contains at least two optical cycles, we see that the time for the envelope to break is always much longer than the breaking time for the carrier. Hence in the situation in which the GVD is very small, the carrier should break before the envelope has enough time to shock. To avoid long computations and accumulation of numerical dispersion errors we have used a Kerr strength of $\chi^{(3)}E_0^2 = 0.01$ ($\delta n = 3\chi^{(3)}E_0^2/8n_0 = 0.0034$), but as

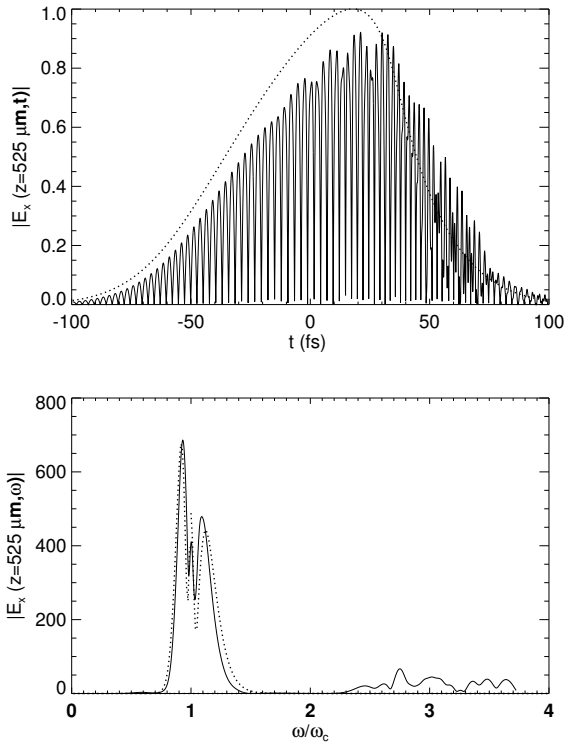

FIG. 4: As in Fig. 3 after propagating 525 microns. An envelope shock has developed on the trailing edge of the pulse which is reflected in the strong spectral broadening in the Fourier spectrum. The third harmonic pulse separates from the fundamental and both fundamental and third harmonic spectra are strongly modulated.

the plot in Figure 2 indicates, the carrier shocking phenomena scales to nonlinear index changes on the order of 10^{-4}. Figure 3 shows a direct comparison of the evolution of an 80 fs pulse for the 1D vector Maxwell and the envelope model (Eq. 10) in a Lorentz medium with a GVD of 2.5 ps^2/km [15] . The envelope solution appears as a smooth curve superimposed on the oscillatory optical carrier pulse solution to Maxwell's equations. The accompanying pulse power spectra show the appearance of a strong third harmonic component characteristic of the carrier shock. Higher harmonics are suppressed by the small GVD present which prevents the carrier wave from breaking as is shown in Figure 1. In Figure 4 the pulse has propagated 525 μm and we see the development of an envelope shock accompanied by the strong spectral broadening and modulation. In the trailing edge one can see the third harmonic pulse generated by the carrier shock is beginning to separate from the fundamental due to the difference in group velocities at the fundamental and third harmonic. For both the carrier and envelope shocks, the GVD prevents the waves from actually breaking. However since the GVD used is quite small, the estimated distances for carrier and envelope shocks (117 μm and 377 μm respectively), are still of use as they indicate the order in which and approximate distances at which the signatures for the shocks appear.

We have shown that novel nonlinear self-steepening effects can act in concert to produce two well separated self-steepening events, one on the optical carrier and the other on the envelope of the carrier (when this is well-defined) as an intense many-femtosecond duration optical pulse propagates in optically transparent media. In the experimental results of Knox et al. [2] the maximum nonlinear index change is 6.4×10^{-3} which is within the range of nonlinearities we have studied (see arrow in Fig. 2). A value of n_2 two orders of magnitude larger than that of silica has recently been reported [16] and is a good candidate material for demonstration of carrier shocks. With the currently available short pulsed lasers one should be able to see the harmonic signature of the carrier shocks even for silica. The standard Sellmeier formula for silica [3, 17] yields a ratio of the phase to group velocity near unity near $\lambda = 620nm$ which is the carrier wavelength used by Knox et al. It is therefore possible that any higher harmonics that they may have observed are in fact the carrier shock signature. The fringe-resolved autocorrelation (FRAC) technique [18] may provide direct measurements of the carrier shock formation. A more realistic model for silica would require our replacing the single resonance Lorentz model with a corresponding three resonance Sellmeier model. This would allow much more flexibility in varying the GVD and the phase-group velocity mismatch.

Acknowledgement: The authors acknowledge support from the Arizona Center for Mathematical Sciences under contract number AFOSR F49620-94-1-0051

[1] *The Supercontinuum Laser Source*, edited by R.R. Alfano, (Springer-Verlag, New York), 1989.
[2] W. H. Knox, R. L. Fork, M. C. Downer, R. H. Stolen, and C. V. Shank, Appl. Phys. Lett. **46**, 1120 (1985).
[3] G. P. Agrawal, *Nonlinear Fiber Optics*, (Academic Press Inc., Boston) 1989.
[4] L. V.Keldysh, Sov. Phys. JETP, **20**, 1307, (1965).
[5] R. M. Joseph, S. C. Hagness and A. Taflove, Optics Letters, **18**, 1412 (1991).
[6] P. M. Goorjian, A. Taflove, R. M. Joseph and S. C. Hagness, IEEE Jou. of Quan. Electr., **28**, 2416 (1992).
[7] P. M. Goorjian and A. Taflove, Optics Letters, **17**, 180 (1992).
[8] R. M. Joseph, P. M. Goorjian and A. Taflove, Optics Letters, **18**, 491 (1993).
[9] Kane S. Yee, IEEE Trans. Antennas Propagat., **AP-14**, 302 (1966).
[10] J. Fang, Ph. D. dissertation, Dept. of Elec. Eng., Univ of

California Berkeley, CA, 1989.
[11] K. L. Shlager et al., IEEE Trans. Antennas Propagat., Vol. 41, 1732-1737, (1993).
[12] P. G. Petropoulos, IEEE Trans. Antennas Propagat., Vol. 42, 859-862, (1994), Vol. 42, 62-69, (1994).
[13] J. D. Jackson, *Classical Electrodynamics*, 2nd ed. (Wiley, New York, 1975)
[14] G. B. Whitham *Linear and Nonlinear Waves*, (Wiley, New York, 1974).
[15] L. G. Cohen, W. L. Mammel, and S. J. Jang, Electron. Lett., **18**, 1023 (1982).
[16] M. Asobe, K. Suzuki, T. Kanamori and K. Kubodera, Appl. Phys. Lett, **60**, 1153 (1992).
[17] D. Marcuse, *Light Transmission Optics*, (Van Nostrans Reinhold, New York, 1982) chaps. 8 and 12.
[18] A. Stingl, M. Lenzner, Ch. Spielmann, and F. Krausz, Optics Letters, **20**, 602 (1995).